

Spin Dynamics in the Two-Dimensional Spin 1/2 Heisenberg Antiferromagnet

A. F. Albuquerque¹, A. S. T. Pires¹, and M. E. G. Souza²

¹Departamento de Física, ICEx, Universidade Federal de Minas Gerais, Belo Horizonte,
CP 702, CEP 30123-970, MG, Brazil,

²Centro Federal de Educação Tecnológica de Minas Gerais, Belo Horizonte, MG, Brazil

(April 20, 2005)

Abstract

We present low-temperature dynamic properties of the quantum two-dimensional antiferromagnetic Heisenberg model with spin $S = 1/2$. The calculation of the dynamic correlation function is performed by combining a projection operator formalism and the modified spin-wave theory (MSW), which gives a gap in the dispersion relation for finite temperatures. The so calculated dynamic correlation function shows a double peak structure. We also obtain the spin-wave damping and compare our results to some experimental data and theoretical results obtained by other authors using different approaches.

PACS numbers: 75.10.Jm ; 67.40.Db ; 75.30.Ds

I. INTRODUCTION

Interest in quantum antiferromagnetism is old and can be traced back to the early years of quantum theory, with Bethe's solution for the Heisenberg antiferromagnetic chain¹. However, research in this field remains very active and was further triggered by the discovery of high-temperature superconductivity in copper-oxide compounds. Superconductivity in the cuprates is attained upon doping the stoichiometric parent compounds, such as La_2CuO_4 , which are believed to be experimental realizations of the two-dimensional quantum Heisenberg antiferromagnet (2D QHAF) with spin $S = 1/2$, described by the Hamiltonian

$$H = J \sum_{\langle i,j \rangle} \mathbf{S}_{\mathbf{r}_i} \cdot \mathbf{S}_{\mathbf{r}_j}; \quad (1)$$

where $J > 0$; $\langle i,j \rangle$ denotes the nearest neighbor (NN) sites on a square lattice, without double counting of bonds. The 2D QHAF can be mapped into the 2D quantum nonlinear model² (2D QNLSM)² and many theoretical works have been dedicated to the investigation of the properties of this last model. However, the mapping is rigorously valid only in the large S continuum limit³, although it can be justified on general grounds for the extreme quantum limit⁴ $S = 1/2$.

The widely held belief that antiferromagnetism plays a central role in high-temperature superconductivity has contributed to a noticeable proliferation of theoretical, numerical, and experimental works devoted to the investigation of the magnetic properties of the stoichiometric parent compounds, as described by (1) and by the 2D NLSM^{5;6}. However, despite this connection with high- T_c superconductivity, the understanding of the properties of the system is important by itself.

Some early theoretical investigations of the 2D QHAF⁷ raised doubts about the nature of the ground state of the model, suggesting that it would be a disordered quantum spin-liquid state with correlations decaying exponentially with distance⁸. Later, further investigations ruled out this possibility and the system is known to exhibit a broken symmetry Neel ground state⁵, which is destroyed by thermal fluctuations⁹ when $T > 0$. In fact, at low tempera-

tures, the system is in a renormalized classical (RC) regime, that is, it behaves as a classical 2D system with coupling constants simply renormalized by quantum fluctuations, as showed by Chakravarty, Halperin and Nelson⁴ in their renormalization-group analysis of the 2D QNLSM. This approach was improved by Hasenfratz and Niedermayer¹⁰ who obtained an expression for the correlation length of the 2D QNLSM in the RC regime which agrees very well with experimental data for the monolayer cuprate $\text{Sr}_2\text{CuO}_2\text{Cl}_2$ ¹¹ over a certain temperature range.

At higher temperatures, $T=J/0.5$, the 2D QNLSM shows a crossover into a quantum critical (QC) region, with correlation length linear in $1/T$ ¹². Although this prediction is difficult to be experimentally tested in cuprates such as $\text{Sr}_2\text{CuO}_2\text{Cl}_2$ and La_2CuO_4 , given the high value of J in these compounds ($J \approx 130\text{ meV}$), recent experiments on copper formate tetradeuterate (CFTD)^{13;14}, which is also described as a 2D QHAF^{15;16} and whose much smaller value of J ($J \approx 6\text{ meV}$) allow measurements up to higher temperatures, found no evidence for a crossover into a QC phase. It should be remarked that the 2D QNLSM is expected to model the 2D QHAF in the limit of low temperatures, when the correlation length is very large, and the above mentioned experiments seem to settle an upper temperature limit for the applicability of this approach. In fact, the validity of the 2D QNLSM approach was shown to be inadequate to describe the behavior of the 2D QHAF with spin value greater than or equal to 1 in the experimentally accessible temperature region¹⁷. For spin $S=1/2$, a series of experiments^{11;18} and Monte Carlo simulations^{19;21} showed that the length scale at which the renormalized 2D QNLSM description becomes valid is surprisingly long. The low energy spectrum of the $S=1/2$ Heisenberg model, obtained by quantum Monte Carlo on finite size lattices²², disagrees rather strongly with the prediction of the non-linear sigma model even when the size of the system is not too small. All these results show that it is important to work directly with Hamiltonian (1) instead of using the 2D QNLSM if one wants to make comparisons with experimental data.

Nowadays, it is believed that the available experimental data for static properties is well described by a combination of low-temperature static properties⁴, QMC simulations^{19;20}

at an intermediate range, and, at higher temperatures, by high-T expansion²¹ and pure-quantum self-consistent harmonic approximation (PQCHA)²³. So, the attention has turned to the dynamical properties of the 2D QHAF at finite temperatures, since the intrinsic nonlinearities in the equations of motion for a spin system give room for stronger quantum effects in the dynamics, particularly at higher excitation energies. Therefore, further microscopic calculations of the dynamic structure factor for (1) are still very welcome in order to allow a better understanding about the system's behavior at finite temperatures.

Many of the interesting phenomena and experimental measurements in strongly correlated quantum systems are related to the dynamics of the system. Despite the considerable progress in many-body theory, available exact results on quantum dynamics in many-body systems are rather scarce. Indeed, even a systematic framework for approximate calculations is not well established²⁴.

In this paper, we calculate the dynamical correlation function for the 2D QHAF with $S = 1/2$ using the equation of motion approach in conjunction with projection operator methods, following a procedure proposed originally by Reiter²⁵ and further developed by other authors²⁶. This method has proven successful in the study of the classical and quantum Heisenberg models in one²⁷ and two²⁸ dimensions showing good agreement with experimental data, Molecular Dynamic simulations and, also, with other theories.

The calculation of the memory function, which plays a central role in the formalism, does not require long-range order to be valid because it depends only on correlations between nearest neighbors. The frequency of the local spin-wave modes is also used as input in the method. The calculation of the static correlations and spin-wave frequency needed in the formalism we are using, is done within the context of the modified spin-wave (MSW) theory proposed by Takahashi²⁹ and Hirsch and Tang³⁰. The MSW theory applied to antiferromagnets imposes a constraint on the total staggered magnetization to be zero in an isotropic system, as required by Mermin-Wagner theorem⁹. It has been shown⁵ that the results obtained via the MSW approximation are identical to the ones obtained by Arovas and Auerbach³² using a path integral formulation in the Schwinger boson representation.

Also, the correlation length, as calculated within MSW theory, agrees with one-loop order in renormalization-group theory for the 2D QNL M⁴.

The combination of these two techniques, the projection operator method and the MSW theory was already applied by some of us³¹ to study the low temperature properties of the quantum one-dimensional Heisenberg model with spin $S = 1$, where a gap is expected to occur.

The dynamical structure function of (1) at finite temperature was firstly calculated by Auerbach and Arovas³³ as the Fourier transform of the imaginary part of the spin-density correlation function

$$S(\mathbf{q}; T) = \frac{1}{\hbar} S^z(\mathbf{q}; T) S^z(-\mathbf{q}; T) \quad (2)$$

using the Schwinger boson mean-field representation. The procedure includes processes where the incident particle creates quasiparticle excitations as well as scattering from thermally excited particles. However, the projection operator method, in the approximation proposed by Reiter²⁵, goes beyond a mean-field theory and, thus, the effects due to magnon scattering are more properly incorporated in the calculation of the dynamical structure factor. This procedure was applied to the 2D QHAF model by Becher and Reiter³⁴, using a standard spin-wave formalism for the calculation of the static quantities, however, as it is well known, conventional spin-wave theory predicts a zero gap value for finite temperatures, i.e., it does not take into account the inexistence of long-range order (LRO) for $T > 0$. More recently, the spin dynamics of the 2D QHAF was investigated by Nagao and Igarashi³⁵ by using the self-consistent theory of Blume and Hubbard³⁶. Their method is expected to work well at high temperatures, although the authors claim that the results obtained for relatively low temperatures, $T = J \approx 0.4$, are reliable because the relaxation function is found to satisfy a dynamical scaling relation consistent with the nonlinear model analysis and, also, Monte Carlo simulations³⁷.

The outline of this paper is as follows: Section (II) gives a brief overview of the MSW results for the spin-wave energy, as obtained by Takahashi²⁹. The steps leading to the

calculation of the dynamical structure factor are also given in this section. In Section (III), we discuss our numerical results and, finally, in Section (IV) we present our conclusions.

II. THE MODIFIED SPIN-WAVE THEORY AND THE PROJECTION OPERATOR METHOD

It is well known that the standard spin-wave theory is not applicable to low-dimensional quantum magnets at finite temperatures without modifications⁹. The consequence of the Mermin-Wagner theorem is enforced by hand in a variational density-matrix approach proposed by Takahashi²⁹, which we will shortly review here. We start our calculations, writing (1) in the form

$$H = J \sum_{\langle ij \rangle} \mathbf{S}_{\mathbf{r}_i} \cdot \mathbf{T}_{\mathbf{r}_j}; \quad (3)$$

where we divide the lattice into two sublattices A and B: spins in sublattice A (B) are denoted as $\mathbf{S}_{\mathbf{r}_i}$ ($\mathbf{T}_{\mathbf{r}_j}$) and the sum runs over all $\mathbf{r}_i \in A$ sublattice sites and its NN on the B sublattice, avoiding double counting of bonds. We now apply a Dyson-Maleev transformation to represent the spin operators in each antiferromagnetic sublattice in terms of bosonic operators

$$\begin{aligned} \mathbf{S}_{\mathbf{r}_i} &= a_{\mathbf{r}_i}^y; \quad \mathbf{S}_{\mathbf{r}_i}^y = (2S - a_{\mathbf{r}_i}^y a_{\mathbf{r}_i}) a_{\mathbf{r}_i}; \\ \mathbf{S}_{\mathbf{r}_i}^z &= S - a_{\mathbf{r}_i}^y a_{\mathbf{r}_i}; \\ \mathbf{T}_{\mathbf{r}_j} &= b_{\mathbf{r}_j}; \quad \mathbf{T}_{\mathbf{r}_j}^y = b_{\mathbf{r}_j}^y (2S - b_{\mathbf{r}_j}^y b_{\mathbf{r}_j}); \\ \mathbf{T}_{\mathbf{r}_j}^z &= S + b_{\mathbf{r}_j}^y b_{\mathbf{r}_j}; \end{aligned} \quad (4)$$

$$\quad (5)$$

following the canonical commutation relations. The Hamiltonian (3) becomes,

$$H = 2NJS^2 + J \sum_{\langle ij \rangle} S \left[a_{\mathbf{r}_i}^y a_{\mathbf{r}_i} + b_{\mathbf{r}_j}^y b_{\mathbf{r}_j} - a_{\mathbf{r}_i} b_{\mathbf{r}_j} - a_{\mathbf{r}_i}^y b_{\mathbf{r}_j}^y + \frac{1}{2} a_{\mathbf{r}_i}^y (a_{\mathbf{r}_i} - b_{\mathbf{r}_j}^y)^2 b_{\mathbf{r}_j} \right]; \quad (6)$$

We then introduce an ideal spin-wave ansatz for the density matrix of the system

$$\rho = \exp \left[-\frac{1}{T} \sum_{\mathbf{q}} \left(\sum_{\mathbf{q}} \left(\frac{y}{\mathbf{q}} a_{\mathbf{q}} + \frac{y}{\mathbf{q}} a_{\mathbf{q}}^\dagger \right) \right) \right]; \quad (7)$$

$\sum_{\mathbf{q}}^{\text{P.O.}}$ indicates summation over half of the first Brillouin zone. $a_{\mathbf{q}}$ and $b_{\mathbf{q}}^y$ are given by the Bogoliubov transformation

$$\begin{aligned} a_{\mathbf{q}} &= \cosh(\epsilon_{\mathbf{q}}) a_{\mathbf{q}} - \sinh(\epsilon_{\mathbf{q}}) b_{\mathbf{q}}^y; \\ b_{\mathbf{q}}^y &= -\sinh(\epsilon_{\mathbf{q}}) a_{\mathbf{q}} + \cosh(\epsilon_{\mathbf{q}}) b_{\mathbf{q}}^y; \end{aligned} \quad (8)$$

where we introduced the Fourier transform of the original boson operators,

$$\begin{aligned} a_{\mathbf{q}} &= \frac{1}{\sqrt{N_A}} \sum_{\mathbf{r}_i} e^{-i\mathbf{q} \cdot \mathbf{r}_i} a_{\mathbf{r}_i}; \\ b_{\mathbf{q}}^y &= \frac{1}{\sqrt{N_B}} \sum_{\mathbf{r}_j} e^{-i\mathbf{q} \cdot \mathbf{r}_j} b_{\mathbf{r}_j}^y; \end{aligned} \quad (9)$$

$N_A + N_B = N$ is the number of sites in the lattice. The dispersion relation, $\epsilon_{\mathbf{q}}$, is obtained after minimizing the free energy with the constraint that the magnetization on each sublattice is zero, $\langle S_x^z \rangle = 0$ and $\langle T_x^z \rangle = 0$, as required by Mermin-Wagner theorem. In this way, we get

$$\begin{aligned} \epsilon_{\mathbf{q}} &= (1 - \cos q_x - \cos q_y)^{1/2}; \\ \epsilon_{\mathbf{q}} &= \frac{1}{2} (\cos q_x + \cos q_y); \end{aligned} \quad (10)$$

We will write the wavevector $\mathbf{q} = (q_x; q_y)$ in units of the inverse lattice spacing.

The parameters α and β can be determined by solving the following set of self-consistent equations,

$$\begin{aligned} S + \frac{1}{2} &= \frac{2}{N} \sum_{\mathbf{q}} \frac{1}{(1 - \cos q_x - \cos q_y)^{1/2}} \frac{1}{2} \coth \left(\frac{\epsilon_{\mathbf{q}}}{2T} (1 - \cos q_x - \cos q_y)^{1/2} \right); \\ \frac{1}{4J} &= \frac{2}{N} \sum_{\mathbf{q}} \frac{\cos q_x}{(1 - \cos q_x - \cos q_y)^{1/2}} \frac{1}{2} \coth \left(\frac{\epsilon_{\mathbf{q}}}{2T} (1 - \cos q_x - \cos q_y)^{1/2} \right); \end{aligned} \quad (11)$$

The same equations have been obtained by Hirsch and Tang³⁰, and, as said before, by Aronov and Auerbach³² in their Schwinger boson treatment.

Takahashi²⁹ was able to find out the asymptotic forms of (11) in the $T \rightarrow 0$ limit and, also, to evaluate the α parameter for the spin $S = 1/2$ case for 4×4 and 64×64 lattices. However, for the calculation of the dynamical structure factor according to the projection

operator procedure, we need to know the spin-wave energy for the infinite square lattice model at finite temperatures and, thus, we solved Eqs. (11) using an iterative numerical model obtaining the results displayed in Table I.

As it is well known, there is no gap in the 2D QHAF with $S = 1/2$ at $T = 0$. Indeed, when $T \neq 0$, we can see that $\beta \neq 1$. However, for finite temperatures, β becomes smaller than unity and so a gap opens in the system, reflecting the fact that the correlation length, ξ , becomes finite and the long wavelength, low-energy spin-waves cannot propagate. So, spin-wave excitations are well defined only for wavelengths significantly smaller than ξ .

Now, we describe only the main steps leading to the calculation of the dynamic structure factor following the projection operator method. A complete description of the theory can be found in Refs. 25,26. One of the advantages of this procedure is that it allows us to obtain the structure factor for all values of the wavevector \mathbf{q} , while calculations based on the nonlinear model are restricted to the long wavelength limit $\mathbf{q} \rightarrow (0;0)$.

In antiferromagnets, spin-waves have two flavors, one associated with the conventional magnetization, $M_{\mathbf{q}} = S_{\mathbf{q}} + T_{\mathbf{q}}$, and another to the staggered magnetization, $R_{\mathbf{q}} = S_{\mathbf{q}} - T_{\mathbf{q}}$, with $\mathbf{r} = x; y; z$. Since the last is a lower energy mode, we will concentrate on the calculation of the dynamical response associated to it. We can see that the staggered magnetization is linear in magnon creation and annihilation operators while the uniform magnetization is a two-magnon operator process. In fact, the calculation of the $M_{\mathbf{q}}$ correlation function could be performed by using the same procedure applied in this work, but the calculation would require us to go to a higher order in magnon operators.

It is important to emphasize that we only calculate rotationally invariant quantities such as $R_{\mathbf{q}} = \frac{1}{3} (R_{\mathbf{q}}^x + R_{\mathbf{q}}^y + R_{\mathbf{q}}^z)$. The Fourier transform of the relaxation function is given by³⁸

$$R(\mathbf{q}; \omega) = \frac{1}{2\pi} \int_{-\infty}^{\infty} dt e^{-i\omega t} \frac{(R_{\mathbf{q}}(t); R_{\mathbf{q}}(0))}{(R_{\mathbf{q}}; R_{\mathbf{q}})} : \quad (12)$$

Here, $(A; B)$ is the Kubo inner product of two operators A and B defined as³⁹

$$(A; B) = \frac{1}{\beta} \text{Tr} e^{-\beta H} A e^{\beta H} B \text{Tr} e^{-\beta H} : \quad (13)$$

where $\langle : : : \rangle$ denotes the usual thermal average and $\beta = 1/k_B T$. One can show that, after some analytical work, the dynamical correlation function $R(\mathbf{q}; !)$ is given by

$$R(\mathbf{q}; !) = \frac{(R_{\mathbf{q}}; R_{\mathbf{q}}) \hbar^2 i \hbar \frac{\omega_{\mathbf{q}}(!)}{!^2 - \hbar^2 i + ! \frac{\omega_{\mathbf{q}}(!)}{!^2} + [! \omega_{\mathbf{q}}(!)]^2}}{(14)}$$

where $\frac{\omega_{\mathbf{q}}(!)}{!^2}$ and $\frac{\omega_{\mathbf{q}}(!)}{!^2}$ are the real and imaginary parts of the second order memory function, $\omega_{\mathbf{q}}(!)$, respectively. In time space, this memory function is expressed by

$$\omega_{\mathbf{q}}(t) = \frac{Q L^2 R_{\mathbf{q}}; e^{-iQ L Q t} Q L^2 R_{\mathbf{q}}}{(L R_{\mathbf{q}}; L R_{\mathbf{q}})} \quad (15)$$

where Q is a projection operator that projects out any term proportional to $R_{\mathbf{q}}$ and $L R_{\mathbf{q}}$, and L is the Liouville operator, defined by the relation $LA = -i[A; H] = -iA$. Reiter²⁵ has shown that, to leading order in temperature, the projection operator Q in the exponential function in (15) can be dropped and we can also write

$$Q L^2 R_{\mathbf{q}} = L^2 R_{\mathbf{q}} - \hbar^2 i R_{\mathbf{q}} : \quad (16)$$

In (14), we also need to define the second frequency moment $\hbar^2 i$, which is given by

$$\hbar^2 i = \frac{(L R_{\mathbf{q}}; L R_{\mathbf{q}})}{(R_{\mathbf{q}}; R_{\mathbf{q}})} : \quad (17)$$

The second time derivatives needed to evaluate the numerator of the memory function (15) are directly obtained from the definition of the Liouville operator and from (3). Since this calculation is very straightforward and the expressions are enormous, we will not show them here. We then apply the Dyson-Maleev (4) and Bogoliubov (8) transformations for the spin operators in those expressions. Doing so, we can simply replace the time evolution $\exp(-iLt)$ by the harmonic time evolution

$$\mathbf{q}(t) = e^{-i!_{\mathbf{q}} t} \mathbf{q}(0) \quad (18)$$

$$\mathbf{y}_{\mathbf{q}}(t) = e^{-i!_{\mathbf{q}} t} \mathbf{y}_{\mathbf{q}}(0); \quad (19)$$

with similar equations for $\mathbf{q}(t)$ and $\mathbf{y}_{\mathbf{q}}(t)$. So, we are left with a number of Kubo products of four bosonic operators which can be decoupled by means of Wick's theorem. After a tedious but simple calculation, we get

$$\chi_q(t) = \frac{4}{N} \sum_p \left[A_+(q;p) \cos(p_+ t) + A_-(q;p) \cos(p_- t) \right] g; \quad (20)$$

$A_+(q;p)$ and $A_-(q;p)$ are given by

$$A_+(q;p) = \frac{2T n_{q_+} n_{q_-} (e^{p_+} + 1)}{4 (1 + e^{p_+}) (1 + e^{p_-}) (LR_{q_+}; LR_{q_-})} [s(q;p) - t(q;p)]^2; \quad (21)$$

$$A_-(q;p) = \frac{2T n_{q_+} n_{q_-} (e^{-p_+} + e^{-p_-})}{4 (1 + e^{p_+}) (1 + e^{p_-}) (LR_{q_+}; LR_{q_-})} [s(q;p) + t(q;p)]^2; \quad (22)$$

where we introduced the notation $q = \frac{q}{2}$ and p , and

$$\begin{aligned} s(q;p) &= \frac{\hbar}{4J^2} (q_+ + q_-) (q_+ + q_- + 2) + \hbar! \frac{2i}{q} (1 + e^{q_+})^{1=2} (1 + e^{q_-})^{1=2}; \\ t(q;p) &= \frac{\hbar}{4J^2} (q_+ + q_-) (q_+ + q_- + 2) + \hbar! \frac{2i}{q} (1 - e^{q_+})^{1=2} (1 - e^{q_-})^{1=2}; \end{aligned} \quad (23)$$

In the expressions above, $n_q = (\exp(-\beta \epsilon_q) + 1)^{-1}$ is the boson occupation number and $s(q;p)$ is defined as

$$s(q;p) = \sum_{q_+} \sum_{q_-} \quad (24)$$

The second moment is readily evaluated from its definition (17). It is given by the ratio of the following expressions

$$(LR_{q_+}; LR_{q_-}) = \frac{4JT}{N} \sum_k \left[2k + k_+ + k_- - \frac{k}{(1 - e^{-2\beta \epsilon_k})^{1=2}} \coth \frac{\beta \epsilon_k}{2T} (1 - e^{-2\beta \epsilon_q})^{1=2} \right]; \quad (25)$$

and

$$(R_{q_+}; R_{q_-}) = \frac{T}{(1 - e^{-\beta \epsilon_q})}; \quad (26)$$

We note that (25) is also needed in the evaluation of equation (21).

If we take the Laplace transform of the memory function (20) and then apply the Cauchy formula we finally get the real and imaginary parts of the memory function as given by

$$\chi_q(\omega) = \frac{1}{2} P \int_{-\infty}^{\infty} d^2 p \left[\frac{A_+(q;p)}{(i\omega + p_+)(q;p)} + \frac{A_+(q;p)}{(i\omega + p_-)(q;p)} + \frac{A_-(q;p)}{(i\omega + p_+)(q;p)} + \frac{A_-(q;p)}{(i\omega + p_-)(q;p)} \right]; \quad (27)$$

and

$$\begin{aligned} \omega_q(\omega) = \frac{1}{2} \sum_{\mathbf{p}} \{ & A_+(\mathbf{q};\mathbf{p}) [\omega + \omega_+(\mathbf{q};\mathbf{p})] + A_+(\mathbf{q};\mathbf{p}) [\omega - \omega_+(\mathbf{q};\mathbf{p})] + \\ & A_-(\mathbf{q};\mathbf{p}) [\omega + \omega_-(\mathbf{q};\mathbf{p})] + A_-(\mathbf{q};\mathbf{p}) [\omega - \omega_-(\mathbf{q};\mathbf{p})] \}. \end{aligned} \quad (28)$$

Comparing equation (20) with the corresponding one obtained by Becher and Reiter (see equation (9) in their paper³⁴), we can note that they are very similar if we assign to ω and $\omega_q(\omega)$ their zero temperature values in our expressions. But there are some slight differences between our definitions for $s(\mathbf{q};\mathbf{p})$ and $t(\mathbf{q};\mathbf{p})$, eqs. (23), and their equivalent ones due to the fact that, in this work, we considered two sub-lattices for the antiferromagnet.

In the next section we discuss our numerical results for the dynamic structure factor calculated from the above expressions.

III. DISCUSSION OF THE NUMERICAL RESULTS

The evaluation of the imaginary part of the memory function is far from trivial. For this purpose, we adopt a numerical method introduced by Gilat and co-workers⁴⁰ and further developed by Wysin⁴¹. A typical result is shown in figure 1, for $(q_x; q_y) = (\pi/2; \pi/2)$, $\beta = T/J = 0.20$; the frequency is given in units of JS^2 (throughout this paper, $k_B = \hbar = 1$). A prominent feature displayed in that figure is that $\omega_q(\omega)$ vanishes in a finite interval approximately centred at the zero temperature spin-wave energy. This can be understood if we look at eq. (28). We can see that we only have contributions when the argument of the delta functions, given by differences or sums of the frequency and the functions $\omega_{\pm}(\mathbf{q};\mathbf{p})$ (which accounts for processes involving an absorption followed by the reemission of a magnon with a lower energy) and $\omega_+(\mathbf{q};\mathbf{p})$ (that describes the decay of a magnon into two others), vanishes. The shape of these two functions is shown in figure 2, also for $(q_x; q_y) = (\pi/2; \pi/2)$ and $\beta = 0.20$. We note that the non-unitary value of β at finite temperatures, a consequence of the absence of long-range order, imposes the opening of a small gap between $\omega_-(\mathbf{q};\mathbf{p})$ and $\omega_+(\mathbf{q};\mathbf{p})$, as we can see in the figure. This gap is close to the zero-temperature spin-wave frequency. So, as we raise the frequency, the two terms involving $\omega_{\pm}(\mathbf{q};\mathbf{p})$ cease to contribute

to the integral in a region where the term in $(\mathbf{q} + (\mathbf{q}; \mathbf{p}))$ still does not contribute, and $\chi_{\mathbf{q}}^{(0)}(\mathbf{q})$ is zero within it. A similar behavior was obtained by some of us in a previous work regarding the dynamics of the $S = 1$ antiferromagnetic chain³¹.

The real part of the memory function is readily evaluated by a generalization⁴² of a numerical method used in one-dimensional cases. In this way, we can directly compute the dynamical correlation function by means of eq. (14). In figure 3, we show the results obtained for $(q_x; q_y) = (\pi/2; \pi/2)$ at $\beta = 0.05, 0.10, 0.15$ and 0.20 . The results for other values of \mathbf{q} are very similar, except for small wave-vectors (such as $(q_x; q_y) = (\pi/64; \pi/64)$) at the highest temperatures studied. In this case, we observe that the imaginary part of the memory function changes its shape, from the normal one as displayed in figure 1 at the lowest temperature investigated ($\beta = 0.05$), into an anomalous one in higher temperatures. This leads to a blurring of the peaks observed in $R(\mathbf{q}; \omega)$. However, this region of small wavevector and high temperature is outside the validity range of the method employed in this work.

We can note that the cancellation of the imaginary part of the memory function in an interval, as discussed above, leads to the vanishing of the dynamic structure factor in the same region. In particular, this feature prevents us to investigate the $\mathbf{q} \rightarrow (0; 0)$ limit, since the gap remains relatively large and there are no peaks in $R(\mathbf{q}; \omega)$. So, we cannot compare our results to those obtained by Becher and Reiter³⁴, who found that the damping of the magnons is zero at $T = 0$.

But, what is remarkable in the curves obtained for $R(\mathbf{q}; \omega)$ is the presence of a double-peak structure. It is interesting to note that the low-energy peak follows the behavior expected for a spin-wave peak, that is, it becomes broader as the temperature increases and its intensity decreases. However, the high-energy peak surprisingly has its intensity increased when we turn up the temperature. One can be tempted to relate this peak to two-magnons excitations, which should become more important when the temperature raises. It is hard to imagine that such a sharp structure defining a double-peak structure will be destroyed if we take into account higher order processes, which are expected to give important contributions

only at high temperatures. A similar structure was also obtained by Auerbach and Arovas³³ in their Schwinger boson treatment of (1). Although we cannot assure that such a result, a double peak structure, is not an artifact of the approximations done, it should be worth to check if such a structure could be resolved in neutron scattering experiments. The same suggestion was made by Auerbach and Arovas.

In order to calculate the damping of the spin-waves, $\gamma(\mathbf{q}; \omega)$, we fit lorentzians to the data points obtained for $R(\mathbf{q}; \omega)$. $\gamma(\mathbf{q}; \omega)$ is so obtained as the halfwidth of the low-energy peak. In figure 4, we show $\gamma(\mathbf{q}; \omega)$ as a function of the wave-vector magnitude along two high symmetry directions in the antiferromagnetic Brillouin zone, for $\beta = 0.05$. We then choose the wave-vector $(q_x, q_y) = (\pi/4, \pi/4)$, indicated in the figure, since this has an intermediate value for the damping, in order to compare the temperature dependence of $\gamma(\mathbf{q}; \omega)$ with the experimental data obtained by Thurber et al.⁴³. We show the results in figure 5. We can see an excellent agreement between our data, indicated by filled diamonds, and the experimental ones, up to a temperature of $T = 350\text{K}$. Also shown in the figure are the previous results by Tyc and Halperin⁴⁴ in their self-consistent calculations and we also see a good agreement between our results.

IV . C O N C L U S I O N S

In summary, we have calculated the dynamic structure factor for the antiferromagnetic Heisenberg model with $S = 1/2$ using a projection operator technique. This approach was also followed by Becher and Reiter³⁴, but they used conventional spin-wave theory in order to calculate the static correlations needed as an input. Instead, we combined the method with the MSW theory, which goes beyond the linear one in the sense that it takes into account the inexistence of long-range order in the model at any finite temperature. We obtained a double-peak structure, as in a previous work of Auerbach and Arovas³³. The damping, calculated by fitting lorentzians to our data points, agrees well with experimental data⁴³ and with previous theoretical calculations by Tyc and Halperin⁴⁴ up to a temperature

T = 350 K .

It is worth to remark that, in the classical limit, the gap will vanish and the double peak structure will disappear. So, the double peak structure found here is a quantum effect.

Huberman et al.⁴⁵ probed the low temperature magnetic excitations of the 2D $S=5/2$ AF compound Rb_2MnF_4 using pulsed inelastic neutron scattering and found a dominant sharp peak that can be identified with one-magnon excitations. However, in addition to this one-magnon peak, he was able to observe a relatively weak continuum scattering at higher energies. This continuum scattering was attributed to scattering by pairs of magnons as expected to happen for the M_q correlation function. This will be the subject of a future work.

Acknowledgements: We acknowledge Takashi Imai for sharing the experimental data shown in figure 5. This work was partially supported by CNPq (Conselho Nacional para o Desenvolvimento Científico e Tecnológico)-Brazil.

REFERENCES

- ¹ H . A . Bethe, Z . Phys. 71, 205 (1931) .
- ² F D M . Haldane, Phys. Rev. Lett. 50, 1153 (1983) .
- ³ I . A eck, Phys. Rev. Lett. 54, 966 (1985); 56, 408 (1986); I . A eck, Phys. Rev. B 37, 5186 (1988) .
- ⁴ S . Chakravarty, B . I . Halperin, and D R . Nelson, Phys. Rev. Lett. 60, 1057 (1988); Phys. Rev. B 39, 2344 (1989) .
- ⁵ E . M anousakis, Rev. M od. Phys. 63, 1 (1991) .
- ⁶ M . A . Kastner, R . J . Birgeneau, G . Shirane and Y . Endoh, Rev. M od. Phys. 70, 897 (1998) .
- ⁷ P W . Anderson, Science 235, 1196 (1987) .
- ⁸ P W . Anderson, M ater. Res. Bull. 8, 153 (1973) .
- ⁹ N . D . M em in and H . W agner, Phys. Rev. Lett. 22, 1133 (1966) .
- ¹⁰ P . H asenfratz and F . N iederm ayer, Phys. Lett. B 268, 231 (1991) .
- ¹¹ M . G reven, R . J . Birgeneau, Y . Endoh, M . A . Kastner, B . K ein er, M . M atsuda, G . Shirane, and T . R . Thurston, Phys. Rev. Lett. 72, 1096 (1994) .
- ¹² A . V . Chubukov, S . Sachdev and J . Ye, Phys. Rev B 49, 11919 (1994) .
- ¹³ H . M . R nnow , D . F . M dM orrow and A . Harrison, Phys. Rev. Lett. 82, 3152 (1999) .
- ¹⁴ P . Carretta, T . C iabattoni, A . Cuccoli, E . M ognaschi, A . R igam onti, V . Tognetti, and P . Verruchi, Phys. Rev. Lett. 84, 366 (2000) .
- ¹⁵ H . M . R nnow , D . F . M dM orrow , R . Coldea, A . Harrison, I . D . Youngson, T . G . Perring, G . A ppli, O . Syljuansen, K . Lefm ann and C . R ischel, Phys. Rev. Lett. 87, 037202 (2001) .

- ¹⁶ Indeed, CFTD can be considered a better realization of a 2DQHAF than the cuprates. In the latter, it was recently pointed the importance of ring exchange in order to fit the experiments. See R. Coldea, S.M. Hayden, G. Aeppli, T.G. Perring, C.D. Frost, T.E. Mason, S.W. Cheong and Z. Fisk, Phys. Rev. Lett. 86, 5377 (2001).
- ¹⁷ A. Cuccoli, V. Tognetti, P. Verruchi, and R. Vaia, J. Applied Phys. 85, 6079 (1999).
- ¹⁸ M. Greven, R.J. Birgeneau, Y. Endoh, M.A. Kastner, M. Matsuda and G. Shirane, Z. Phys. B 96, 465 (1995).
- ¹⁹ B.B. Beard, R.J. Birgeneau, M. Greven and U.-J. Wiese, Phys. Rev. Lett. 80, 1742 (1998).
- ²⁰ J.-K. Kim and M. Troyer, Phys. Rev. Lett. 80, 2705 (1998).
- ²¹ N. Elstner, A. Sokol, R.R.P. Singh, M. Greven and R.J. Birgeneau, Phys. Rev. Lett. 75, 938 (1995).
- ²² C. Lavalie, S. Sorella, and Alberto Parola, Phys. Rev. Lett. 80, 1746 (1998).
- ²³ A. Cuccoli, V. Tognetti, R. Vaia and P. Verruchi, Phys. Rev. Lett. 77, 3439 (1996).
- ²⁴ Y. Maeda, K. Sakai, and M. Oshikawa, cond-mat/0501295.
- ²⁵ G. Reiter and A. Sjölander, Phys. Rev. Lett. 39, 1047 (1977); G. Reiter, J. Phys. C: Solid State Phys. 13, 3027 (1980).
- ²⁶ B. De Raedt, H. De Raedt, and J. Fizez, Phys. Rev. B 23, 4597 (1981); Phys. Rev. Lett. 46, 786 (1981).
- ²⁷ M.E. Gouvea and A.S.T. Pires, J. Phys. C 20, 2431 (1987).
- ²⁸ S.L. Menezes, A.S.T. Pires, and M.E. Gouvea, Phys. Rev. B 47, 12280 (1993).
- ²⁹ M. Takahashi, Phys. Rev. B 40, 2494 (1989).
- ³⁰ J.E. Hirsch and S. Tang, Phys. Rev. B 40, 4769 (1989); S. Tang, M.E. Lazzouni, and J.E.

- Hirsch, Phys. Rev. B 40, 5000 (1989).
- ³¹ A. S. T. Pires and M. E. Gouvêa, J. Mag. Mat. 241, 315 (2002).
- ³² D. P. Arovas and A. Auerbach, Phys. Rev. B 38, 316 (1988).
- ³³ A. Auerbach and D. P. Arovas, Phys. Rev. Lett. 61, 617 (1988).
- ³⁴ T. Becher and G. Reiter, Phys. Rev. Lett. 63, 1004 (1989); Phys. Rev. Lett. 64, 109 (1990).
- ³⁵ T. Nagao and J. Igarashi, J. Phys. Soc. Jpn. 67, 1029 (1998).
- ³⁶ M. Blume and J. Hubbard, Phys. Rev. B 1, 3815 (1970).
- ³⁷ M. Makić and M. Jarrell, Phys. Rev. Lett. 68, 1770 (1992).
- ³⁸ A. S. T. Pires, Helv. Phys. Acta 61, 988 (1988).
- ³⁹ H. Mori, Prog. Theor. Phys. 34, 399 (1965).
- ⁴⁰ G. Gilat and J. Raubenheimer, Phys. Rev. 144, 390 (1966); G. Gilat and Z. Kam, Phys. Rev. Lett. 22, 715 (1969); G. Gilat, J. Comput. Phys. 10, 432 (1972).
- ⁴¹ G. M. Wysin, private communication (1998).
- ⁴² G. M. Wysin, private communication (1999).
- ⁴³ K. R. Thurber, A. W. Hunt, T. Imai, F. C. Chou and Y. S. Lee, Phys. Rev. Lett. 79, 171 (1997).
- ⁴⁴ S. Tyc and B. I. Halperin, Phys. Rev. B 42, 2096 (1990).
- ⁴⁵ T. Huberman, R. Coldea, R. A. Cowley, D. A. Tennant, R. L. Leheny, R. J. Christianson, C. D. Frost, cond-mat/0504684.

TABLES

T /J		
0.05	0.999999993	2.609963279
0.10	0.999995178	2.609876929
0.15	0.999939299	2.599595679
0.20	0.999709621	2.562049716
0.25	0.999280433	2.567211935
0.30	0.998523449	2.558794763

TABLE I. Results for the α and β parameters for some temperatures T used in our calculations. The values were obtained by solving Eqs (11) numerically.

FIGURES

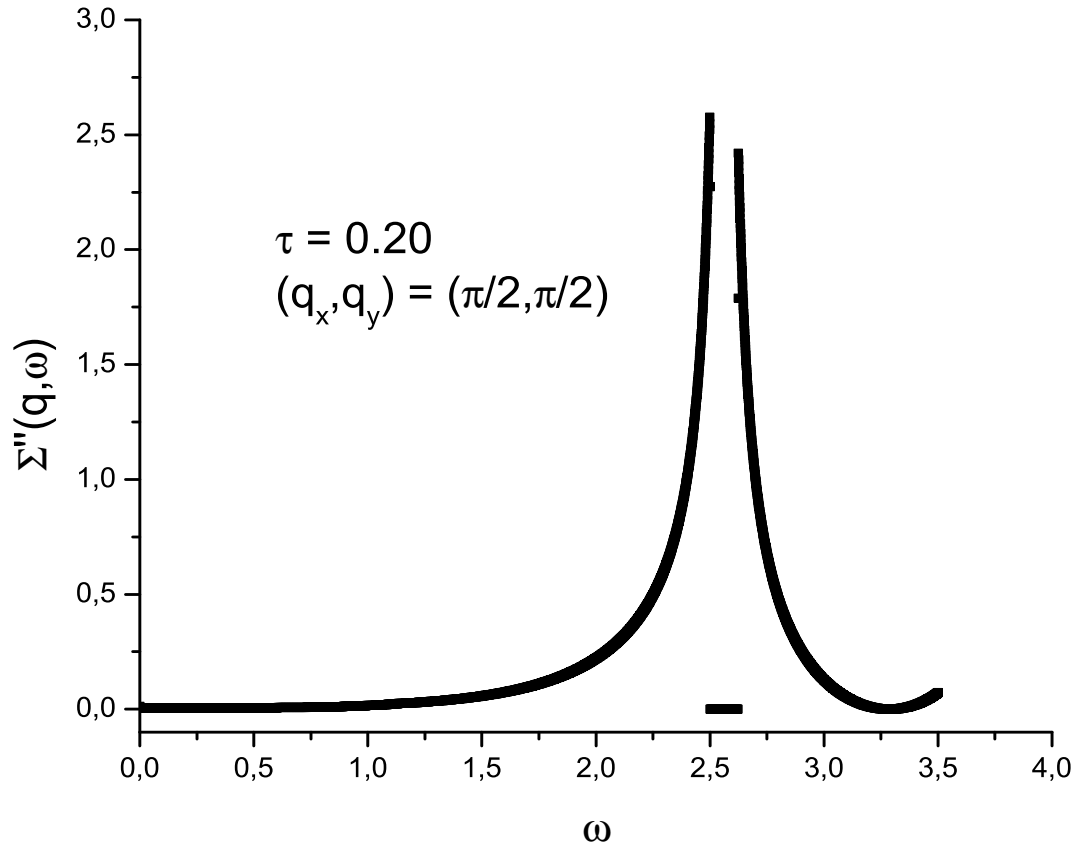


FIG. 1. Imaginary part of the memory function, $\Sigma''_{\mathbf{q}}(\omega)$, as a function of ω for $(q_x, q_y) = (\pi/2, \pi/2)$ and $\tau = 0.20$.

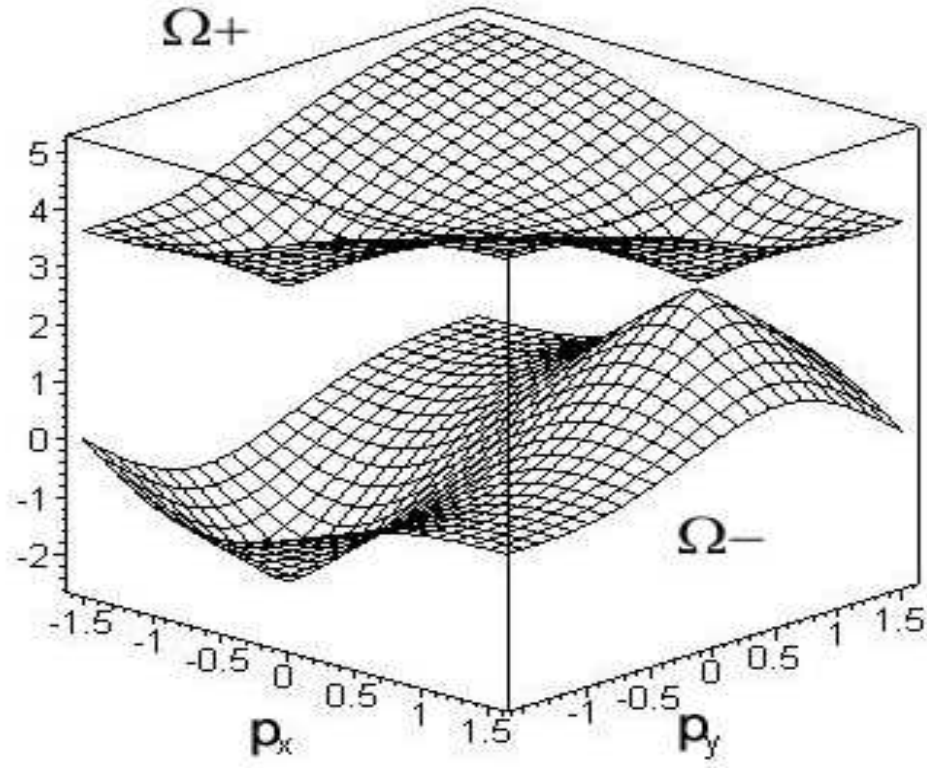


FIG .2. $(\mathbf{q};\mathbf{p})$ and $+(\mathbf{q};\mathbf{p})$ as a function of $(p_x;p_y)$ for $(q_x;q_y) = (\pi/2;\pi/2)$ and $\hbar = 0.20$.

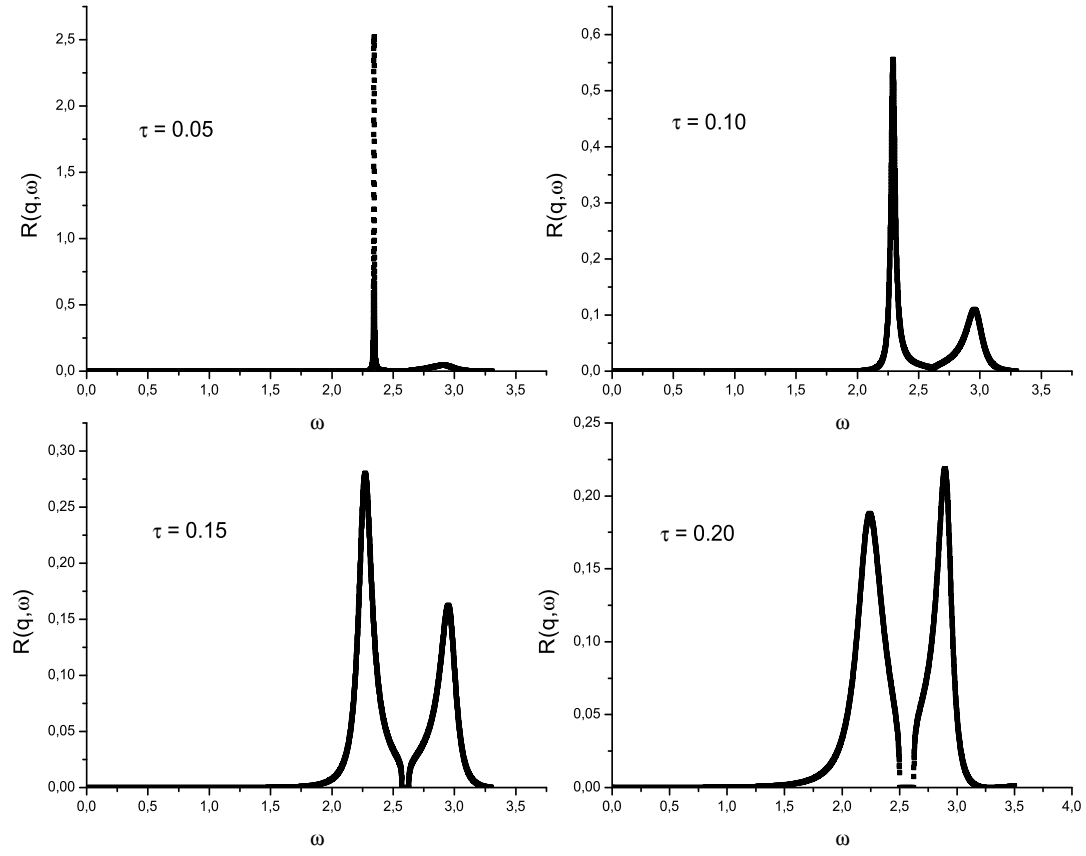


FIG. 3. Dynamic structure factor, $R(q; \omega)$, for $(q_x; q_y) = (\pi/2; \pi/2)$ and $\tau = 0.05, 0.10, 0.15$ and 0.20 .

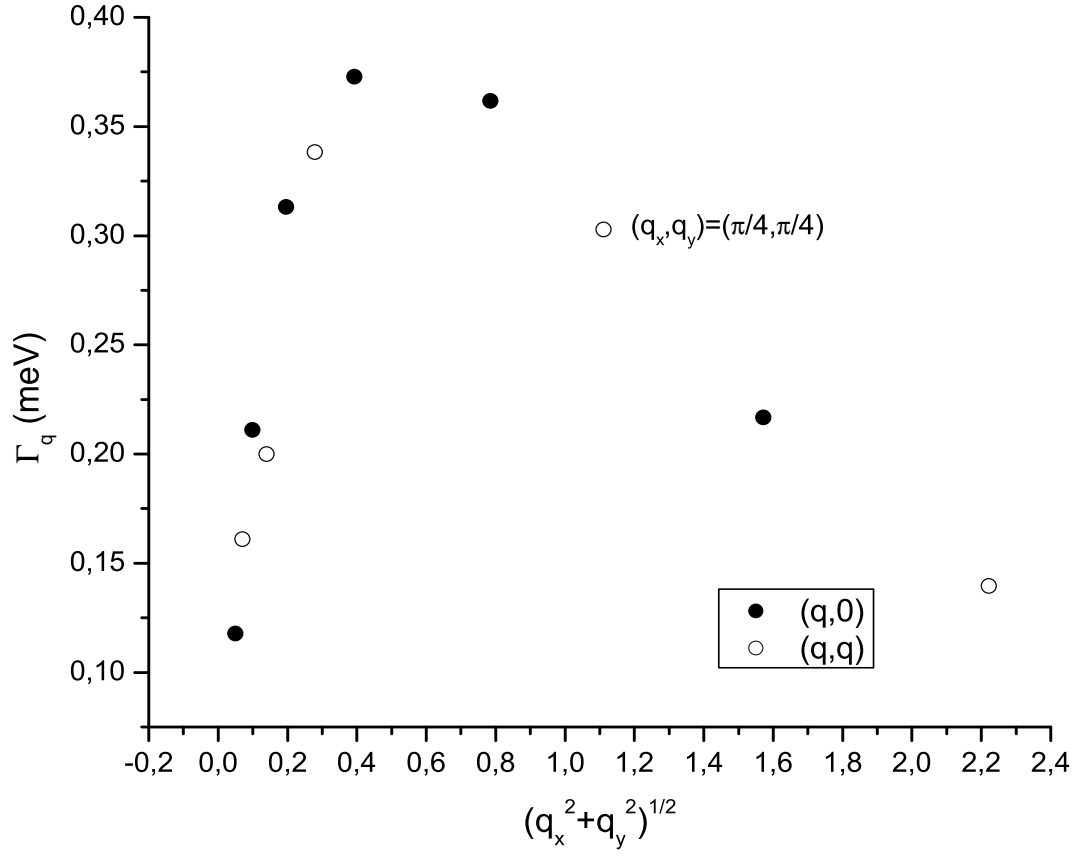


FIG . 4. Results obtained in our work (as explained in the text) for the spin-wave damping, Γ_q , as a function of $(q_x^2 + q_y^2)^{1/2}$ for $\alpha = 0.05$. Filled circles are for wavevectors along the direction $(q;0)$ and open circles for $(q;q)$. Wave-vector $(q_x; q_y) = (\pi/4; \pi/4)$ is indicated.

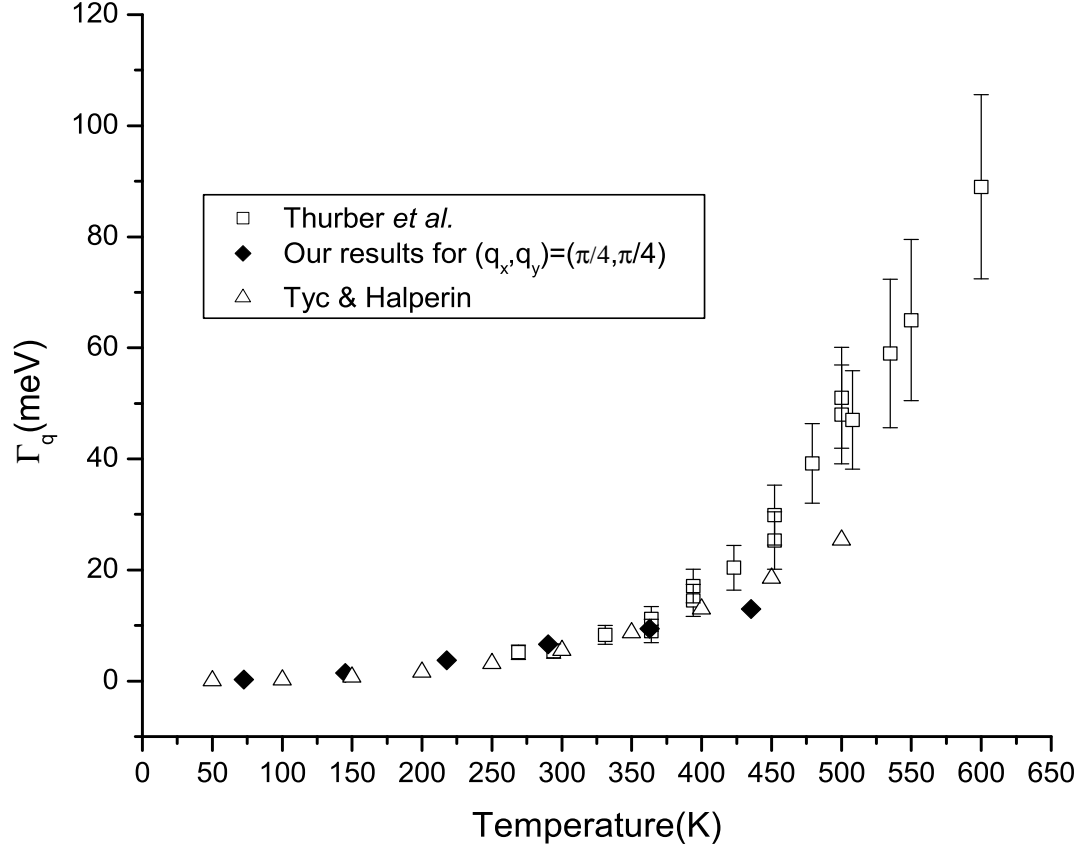


FIG. 5. Spin-wave damping, Γ_q , as a function of temperature for $(q_x, q_y) = (\pi/4, \pi/4)$ (filled diamonds). Open squares are the experimental results from Thurber *et al.*,⁴³ and open triangles are theoretical results from Tyc and Halperin⁴⁴.